Study of Impact Type Surface Junction Thermocouple

Journal of Propulsion and Energy Vol. 1, No. 1. October 2020; 1(1): 74-84
https://doi.org/10.6108/JPNE.2020.1.1.074
pISSN 2734-1887 eISSN 2765-0049

JPNE

Study of Impact Type Surface Junction Thermocouple

Sangha Park [a] · **Gisu Park** [a,*]

[a] Department of Aerospace Engineering, Korea Advanced Institute of Science and Technology, Daejeon 34141, Korea

Corresponding author [*]
Gisu Park
gisu82@kaist.ac.kr

Received : 19 March 2020
Revised : 4 September 2020
Accepted : 8 September 2020

In this study, a coaxial thermocouple subjected to impact through a junction manufacturing process was investigated. The performance of the impact-type coaxial thermocouple was analyzed through impact and thermal tests to evaluate the resistance of the thermocouple to external forces and heat. In addition, shock tunnel experimental tests were conducted to assess the durability of the thermocouple in a hypersonic environment. The findings indicated that the impact-type coaxial thermocouple exhibited satisfactory resistance to external heat. Moreover, the results exhibited sufficient repeatability, and the performance of the impact-type coaxial thermocouple was determined to be comparable to that of the conventional coaxial thermocouple.

Key Words: Shock tunnel, Thermocouple, Surface junction

Nomenclature

F	Force (N)
P	Pressure (Pa)
T	Temperature (K)
q	Heat flux (W/m^2)
TP	Thermal product $(W \cdot sec^{1/2}/[m^2 \cdot K])$
ρ	Density (kg/m^3)
C_p	Specific heat at constant pressure $(J/[kg \cdot K])$
k	Thermal conductivity $(W/[m \cdot K])$
R	Resistance (Ω)
t	Time (sec)

Subscript

a	Ambient
w	Water
s	Surface
∞	Freestream

1. Introduction

Shock tubes [1-4] and shock tunnels [5-11] are typical high-speed ground test equipment, and they have the advantage over other equipment in simulating various types of flow. However, the disadvantage of using them is that the test flow time is very short in milliseconds, and the sensor may be destroyed because of direct impact owing to debris from the diaphragm [12]. Therefore, the heat sensor used in shock tubes or shock tunnels should show fast response times, and it should resist harsh environmental conditions within the test equipment. Coaxial surface junction thermocouples are widely used in hypersonic ground test experiments, such as shock tunnel [13,14]. Figure 1 shows a K-type coaxial thermocouple and its measurement schematic. A coaxial thermocouple comprises a combination of a central alumel alloy bar and a central-pierced chromel alloy cylinder. Between the alumel bar and the chromel cylinder, an insulator is placed to prevent current from flowing. The outside part of the thermocouple, except the contacts, is also covered with insulators for mounting the model.

Typically, a coaxial thermocouple is manufactured by hand, the junction generation process depends on experience and skill [15,16]. In the grind-type thermocouple, a random junction that is generated by scratching the surface using sandpaper causes a difference in the way each sensor functions. In addition, araldite adhesive and teflon tape, which are commonly used as adhesives between metals, may have weak thermal and shock drawbacks, so it is possible that the thermocouple suddenly experiences sudden pressure and thermal changes in the hypersonic test facility environment.

In this study, an impact-type coaxial thermocouple was studied to address the junction imbalance that exists between thermocouples. The impact and thermal performance of the impact-type thermocouple were investigated in a hypersonic environment in a shock tunnel. The results of the shock tunnel test were compared with the findings for a similar condition reported in Ref. [12]. The heat flux of the impact-type surface junction thermocouple compared favorably with that of the conventional grind-type thermocouple, which verified the study results and demonstrated the potential for the use of impact-type surface junction thermocouple.

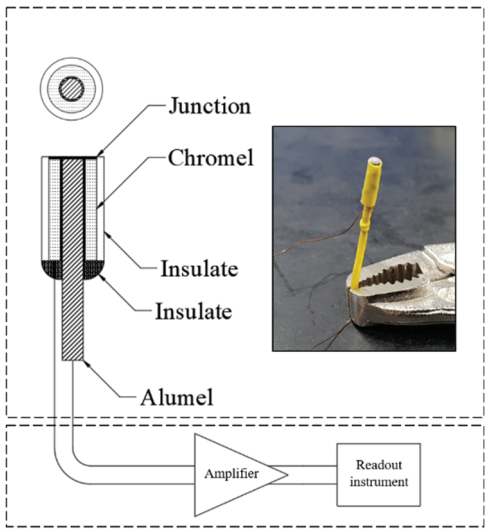

Fig. 1. Schematic of a k-type coaxial surface junction thermocouple.

2. Experimental Details

2.1 Thermocouple

Coaxial thermocouples are usually fabricated by hand. Typically, the junction manufacturing process is achieved using sandpaper [17-24] or by scratching the surface using a scalpel [25,26] for random plastic deformation of the thermocouple surface. A tapered rod is used to improve the process further [25,27]. The application of the tapered method involves using an outside tapered rod for manufacturing the junction on the surface instead of using the conventional straight rod. However, this method usually requires a unique manufacturing technique in which microscopic manufacture for the tapered rod is necessary. Sandpapers are widely used for creating the junction in hand-made coaxial thermocouples. The

grind-type junction fabrication is generally used for thermocouple production.

In this study, a thermocouple manufacturing process of applying impact force was studied. A thermocouple that is produced following the further manufacturing process is called an impact-type coaxial surface junction thermocouple. Unlike the conventional junction fabrication process that involves sandpaper grinding or the use of a sharp scalpel, the manufacturing process for the impact-type coaxial surface junction thermocouple requires a surface impact to make the surface junction durable. The junction fabrication of the grind-type or scalpel-type thermocouple includes the microscopic distortion of the overall surface. However, the junction fabrication process of the impact-type thermocouple is focused on durable local distortion.

Figure 2 depicts the manufacturing process and schematic of the impact-type coaxial thermocouple. A K-type thermocouple, which was composed of two different metallic substances, was used in this study. The first metallic material was chromel alloy, which consisted of 90% nickel and 10% chrome. The other material was alumel alloy, which consisted of 95% nickel, 2% aluminum, 2% manganese, and 1% silicon. The initial process was similar to that of the conventional grind-type thermocouple; an alumel alloy rod and a chromel alloy cylinder were glued together using an insulation material and araldite adhesive. A copper wire was then attached to the sensor, and surface insulation was applied using a teflon tape. Next, sandpaper with grit sizes of 800 to 1500 was used to smoothen the surface. Thereafter, the thermocouple was fixed to the vise after surface treatment, and contact was created by placing a sharp object about the

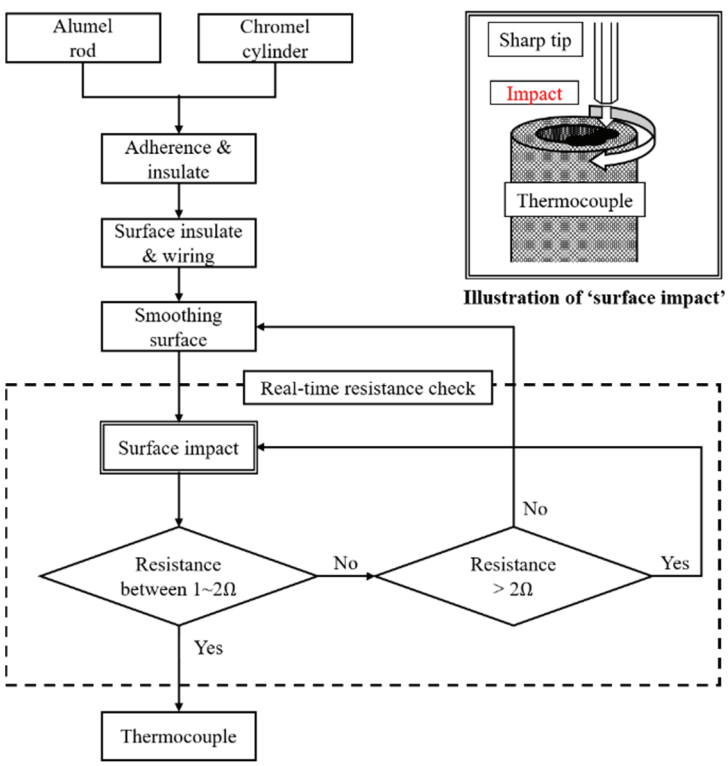

Fig. 2. Logic scheme of impact type surface junction thermocouple manufacture.

size of an M3 hexagonal wrench on the surface and striking the object with a hammer. The thermocouple was usable when the resistance was 1–2 Ω. When the measured resistance exceeded 2 Ω, contact initiation was achieved through impact junction application. However, when the resistance was lower than 1 Ω, then the thermocouple could not be used in the hypersonic environment because the sensitivity was unavailable in the hypersonic ground test facility. The junction was removed by via surface smoothing, and the thermocouple became reusable. The processes of creating contact through impact and checking the resistance were evaluated in real-time by connecting a resistor to a wire that was attached to the thermocouple. When the resistance was within the optimal range of 1–2 Ω, the thermocouple could function effectively without further processing.

2.2 Calibration

Calibration was performed to determine the sensitivity of the heat flux before the thermocouple could be used. In this study, a widely used method for thermocouple calibration, known as the water plunging method, was used [26]. Figure 3 shows the setup for the water plunging method, i.e., the calibration technique and the schematic. The thermocouple for calibration was connected to the support and located on ice water. The reason for using ice water is to protect thermocouples from the steam of hot water. The wire attached to the thermocouple was connected to an oscilloscope through the amplifier and measured the voltage generated by the thermocouple.

The calibration method is described as follows. The surface temperature of the thermocouple was measured, and the thermocouple was suddenly dropped into a bowl of ice water maintained at a temperature close to 273 K. At this point, the sudden change in temperature was measured using the oscilloscope. The measured temperature difference can be related to the thermal product (TP) using equation (1) [28]:

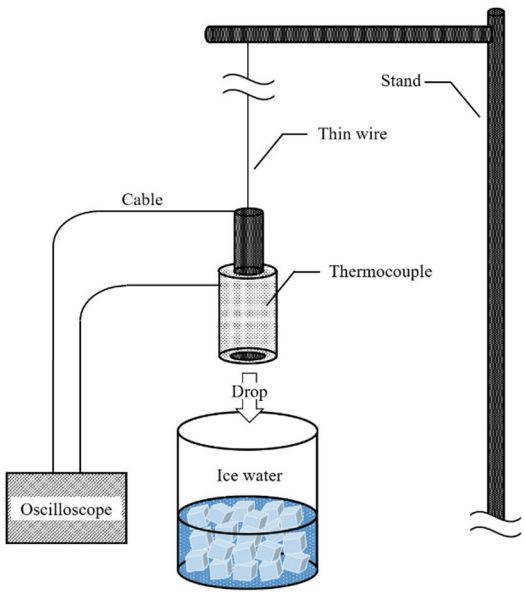

Fig. 3. Thermocouple calibration setup.

$$\frac{T - T_a}{T_w - T_a} = \frac{(TP)_w}{(TP)_w + TP} \tag{1}$$

In equation (1), $\mathrm{TP} = \left(\rho C_p k\right)^{1/2}$ is the thermal product of the thermocouple, T is temperature, the subscripts a, s and w denote ambient, surface of the thermocouple, and water, respectively. The thermal product of water is expressed as $(\mathrm{TP})_W = 1592\ \mathrm{Ws}^{1/2}/\mathrm{m}^2\mathrm{K}$ at 273 K, based on the regression of Ref. [29]. The thermal product of each thermocouple $(\mathrm{TP})_s$ can be obtained through the calibration.

In this study, the experimental tests were conducted at $T_a = 293K$. The calibration was performed by securing the thermocouple surface temperature with $T_W = 273\ K$ using ice water. Calibration was performed five times, and the average thermal product was used. Figure 4 shows a sample of the calibration results obtained using the water plunging method. When the thermocouple was immersed in the water, a sudden temperature change was detected within approximately 1 msec, and the temperature remained constant thereafter. The value of the thermal product of the thermocouple obtained in this study was 6361 $W \cdot sec^{1/2}/[m^2 \cdot K]$.

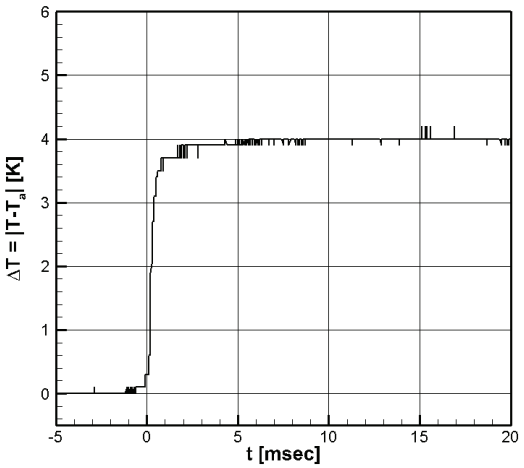

Fig. 4. Typical variation of surface temperature against time.

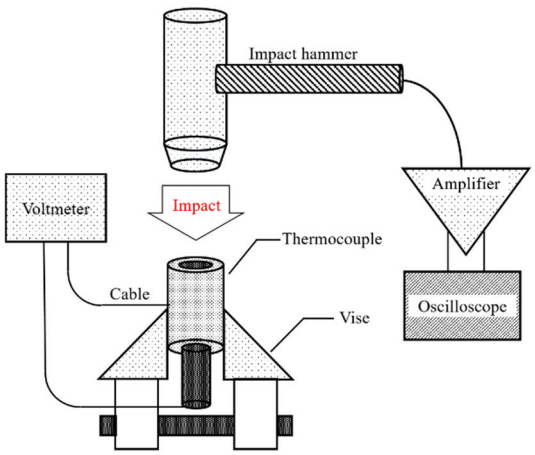

Fig. 5. Impact resistance test setup.

2.3 Impact and Thermal Durabilities

Thermocouple impact durability tests were conducted to observe the degree of resistance variation, which is a measure of the junction generation for subsequent thermocouple by directly impacting the thermocouple surface. Figure 5 shows the appearance and describes the aim of performing the impact durability test. The impact durability test process involved fixing the thermocouple to a vise and applying impact. A fixed thermocouple was connected to a voltmeter, which facilitated the real-time observation of the thermocouple resistance changes before and after impact. The impact of the impact hammer (PCB Piezotronics, Model 086C01) on the thermocouple was observed using the oscilloscope connected to the amplifier. The impact was measured in volts and could be converted to newtons using the calibration data provided. In this study, the plastic tip of the impact hammer was used, which resulted in a voltage versus impact variation of 10.36 mV/N. The impact force after each trial and the thermocouple resistance were obtained to analyze the changes in the thermocouple.

Thermocouple thermal durability tests were performed to examine the degree of resistance variation. The tests were designed to simulate thermocouple exposure to temperature in a shock tube/ shock tunnel, and a sudden increase in temperature occurred after the shock reached that of the model.

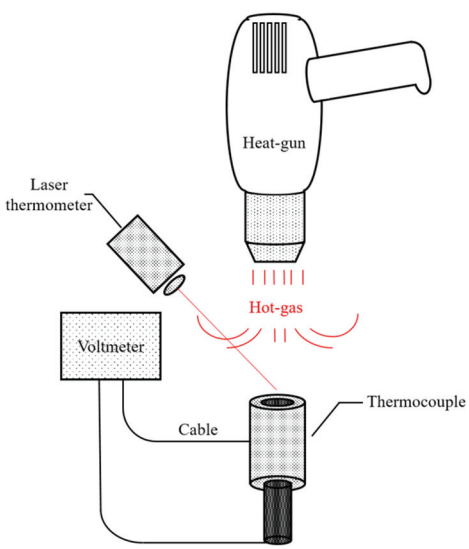

Fig. 6. Thermal resistance test setup.

An experiment was conducted to measure thermocouple junction variations by applying heat to the surface of each thermocouple model. The junction variations were observed by measuring the junction resistance after the application of the heat. Figure 6 shows the experimental setup for the thermal durability test. A heat gun was used to heat the thermocouple surface, and the temperature was measured using a laser thermometer. After the heat was applied for 5 sec successively at intervals, the change in junction was measured through the change in resistance based on the thermocouple surface temperature.

2.4 Shock Tunnel Experiment

Figure 7 shows the setup for the shock tunnel tests. The experimental tests were conducted using a K1 shock tunnel located at KAIST. This shock tunnel was composed of a Mach 6 contour nozzle. Models and thermocouples mounted in the test section were connected to the amplifier and the oscilloscope using a cable to measure the temperature change in a hypersonic environment. After each shock tunnel test was performed, the thermocouple resistance was measured using a voltmeter to determine the change in the thermocouple junction between each experimental process.

The measured temperature change was calculated based on the heat flux using the semi-infinite technique expressed in equation (2) [30].

$$q(t_n) = \frac{2(\rho C_p k)^{\frac{1}{2}}}{(\pi)^{\frac{1}{2}}} \sum_{i=1}^{n} \frac{T(t_i) - T(t_{i-1})}{(t_n - t_i)^{\frac{1}{2}} + (t_n - t_{i-1})^{\frac{1}{2}}} \quad (2)$$

In equation (2), t is time. The thermal product $(\rho C_p k)^{1/2}$ was determined during the calibration process.

Figure 7-(b) and (c) show the pitot pressure and the heat

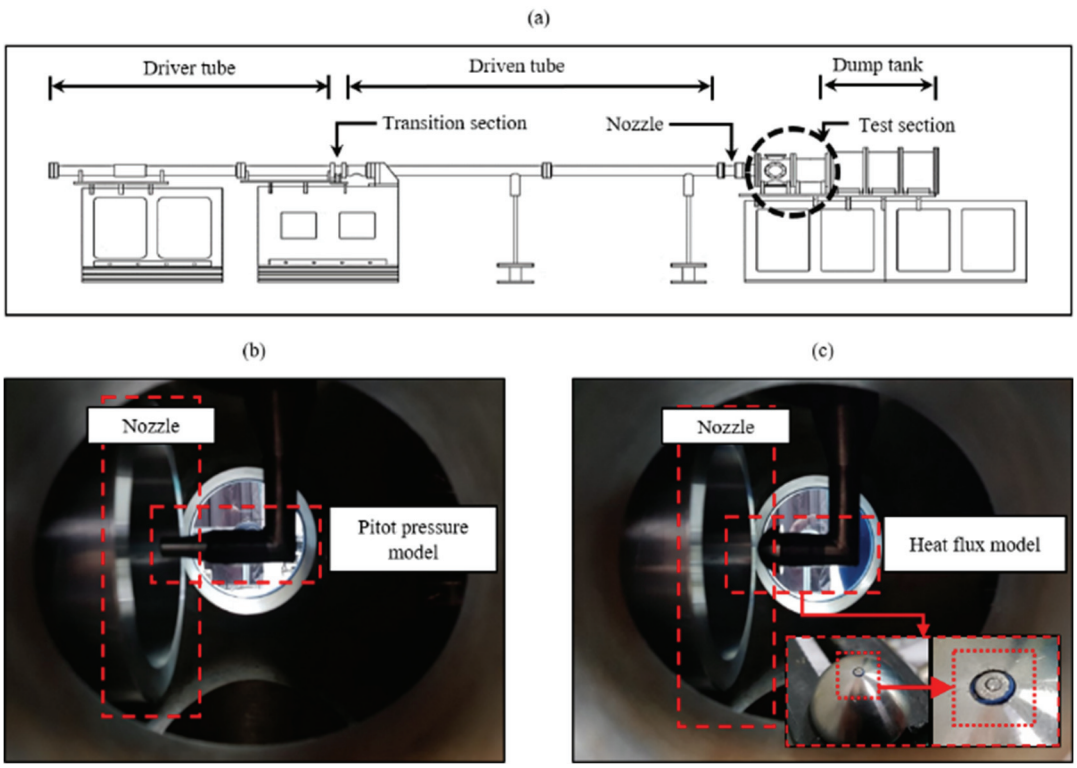

Fig. 7. Shock tunnel experiment. (a) Test facility; (b) Pitot pressure model; (c) Heat flux model.

flux models equipped. A hemisphere model having a diameter of 30 mm was used to equip the coaxial thermocouple. The thermocouple was equipped to match the model surface. The model was equipped with a L-shaped model anchorage and a test section, with the thermocouple wires projecting outward through the inner space of the anchorage.

The charging conditions of the shock tunnel were similar to the flow conditions used in Ref. [12]. Helium and nitrogen (at 3.2 ±0.05 MPa) were pre-mixed and used as the charging gases for the driver to increase the experiment time through driver gas tailoring. At the transition section, 1.66 ±0.01 MPa of helium was used, whereas 40 kPa of dry air was used in the driven tube. The nitrogen inside the driver tube did not strongly affect the flow condition in the test section [31]. The considered shock tunnel condition at the nozzle exit was as follows: the freestream pressure (P_∞) was 1.73 kPa; the temperature (T_∞) was 200 K; and the density (ρ_∞) was 0.03 kg/m^3. Detailed information regarding the calculation procedure of flow condition can be found in Ref. [31].

The obtained heat flux and pitot pressure measurement results were compared with the data presented in Ref. [12] to ensure that the results obtained in this study could be verified for similar conditions.

3. Results and Discussion

3.1 Impact and Thermal Durabilities

Table 1 shows the degree of resistance variation measured from the impact durability tests and the maximum impact at each time. The impact of the hammer between each attempt was adjusted to approximately 70–130 N. As inferred from the resistance change following each attempt (Table 1), the impact-type thermocouple showed a continuous increase in resistance to surface impact. To the authors' understanding, a plastic transformation of surface occurs through the impact, and hard junctions are formed between the materials. However, as the impact is applied, there seems to be some influence on the amount of plastic transformation of the surface but upto several trials, the survivability of the thermocoupole seems fair at best.

Table 2 shows the resistance change between each attempt through thermal durability tests and the thermocouple surface temperature measured using a laser thermometer. The thermocouple surface temperature values listed in the table are indicated by the maximum measured temperature, considering the continuous heating of the thermocouple surfaces for a duration of 5 sec. The maximum temperatures of the surfaces ranged from 330–340 K.

In contrast to the impact durability test results, the thermocouple showed a steady difference of ±0.4 Ω for each heating process. This result suggested that for the impact-type thermocouple, the contact between the alumel rod and the chromel cylinder through direct surface deformation was likely to be less affected by the insulating material.

Table 1. Variation of surface resistance against applied force.

Trial	F_{max} (N)		R (Ω)	
#0	-		1.5	
#1	96.5		2.3	
#2	77.2		2.2	
#3	127.4		2.8	
#4	100.4		2.6	
#5	81.2	±0.4	3.6	±0.05
#6	123.6		3.3	
#7	61.8*		4.2	
#8	81.1		4.4	
#9	92.7		4.5	
#10	77.2		5	

Table 2. Variation of surface temperature and resistance against applied heat.

Trial	T_s (K)		R (Ω)	
#0	-	±1.4	1.4	±0.05
#1	338.5		1.1	
#2	335.3		1.2	
#3	336.5		1	
#4	337.6		1.4	
#5	334.2		1.6	

3.2 Shock Tunnel Experiment

Figure 8 shows the heat flux and pitot pressure results of the shock tunnel tests. From Figure 8-(a), the average value of pitot pressure was 80±2.3 kPa, compared with the theoretical value of 81 kPa. Thus, the obtained pitot pressure results were in good agreement with the theoretical value. The experimental condition of Ref. [12] as similar to the flow condition used in this study, so data were selected for comparing and verifying the results. In Ref. [12], the pitot pressure was 85±1.7 kPa; the results for pitot pressure obtained in the present study also exhibited satisfactory agreement with the results in the reference.

The results for the temperature and heat flux of the impact-type thermocouple determined through shock tunnel tests are shown in Figure 8-(b), Figure 8-(c), and Table 3. From Figure 8-(b), in all the five trials, the temperature changed with time and showed a similar trend. Based on the thermocouple resistance variations presented in Table 3, at a resistance variation of approximately 0.3 Ω, the sensitivity of thermocouple barely changed. In Figure 8-(c), the impact-type thermocouple showed a steady time of 2 msec for all the trials. Compared with Figure 8-(a), the measured heat flux followed a steady time range for pitot pressure, and the steady time ended similarly to that of the pitot pressure approximately 2.5 msec after the shock wave arrived. The steady time for heat flux also followed a steady time for pitot pressure, i.e., approximately 2 msec of steady time start and end, similar to that of pitot pressure. The heat flux measured at each trial had an average value of $1.37 \pm 0.02\ \mathrm{MW/m^2}$. As can be seen from Figure 8 and Table 3, the heat fluxes measured in all the trials exhibited similar shapes and values. In Ref. [12], a conical nozzle with a designed Mach number of 6.08 were used. In this study, a contour nozzle having a Mach number of 6 was used, and the driver gas tailoring technique was adapted to increase the test time. The measured test time reported in Ref. [12] was shorter (steady time of approximately 0.5 msec) than the test time of this study (steady time of 2–2.5 msec). For shock tunnel tests, both a 5% increase in pitot pressure and a 12.7% increase in heat flux were obtained then that of Ref. [12]. A possibility for the differences may be the difference between the conical nozzle and contour nozzle used. The designed Mach number of the contour nozzle was slightly lower than that of the conical nozzle used. The differences in the Mach number and freestream conditions between the conical and contour nozzles may have caused the higher pressure and heat flux obtained in this study.

Another possible reason for the difference in the surface

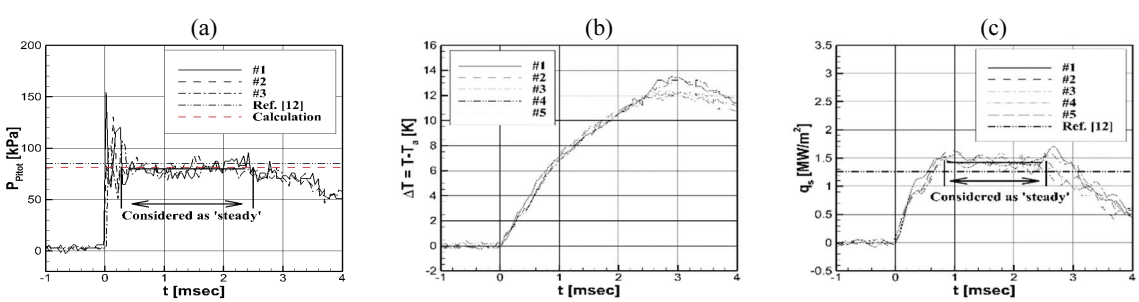

Fig. 8. Measured shock tunnel data. (a) Pitot pressure; (b) Temperature; (c) Surface heat flux.

heat flux may be the roughness variance between the models. In this study, a hemisphere model similar to that of Ref. [12] was used. However, unlike the factory release smooth model used in the reference, the model used in this study had a rather rough surface. Based on previous studies, heat flux tends to be higher for a rough surface. In Ref. [4] and Ref. [32], it was shown that the surface heat flux for rough surfaces was up to 20% higher than those of smooth surfaces.

Table 3 shows the thermocouple resistance variation and the measured average heat flux value for each trial. The results, which showed different results for the impact and thermal durability tests, suggested that it had a steady performance in the experimental condition. Characteristically, during the impact durability tests, the thermocouple resistance showed a steady rise after each trial. However, the shock tunnel test results showed a similar trend with the thermal durability test results, and the steady resistance variation was up to $\pm 0.3\ \Omega$. In this regard, the impact-type surface junction thermocouple performed quite well.

Table 3. Surface heat flux data comparison.

Trial	q (MW/m^2)		R (Ω)		q (MW/m^2) (Ref. [12], Conventional type)	
#0	-	±0.02	1.3	±0.05	1.26	±0.03
#1	1.40		1.5			
#2	1.38		1.4			
#3	1.40		1.4			
#4	1.32		1.5			
#5	1.36		1.6			

4. Conclusions

In this study, the impact-type thermocouple was experimentally investigated. The performance of the impact-type thermocouple was evaluated by determining the impact and thermal durabilities of the thermocouple as well as its durability in the shock tunnel tests. Based on the impact and thermal durability results, the impact-type coaxial thermocouple showed good thermal resistance but a rather low impact resistance. From the shock tunnel experimental tests, the results suggested that the impact-type thermocouple exhibited steady performance in terms of repeatability. The resistance variations for the shock tunnel tests were measured, and the maximum difference observed was $\pm 0.3\ \Omega$, which indicated steady repeatability, with reasonable heat flux measurement capability indicating the efficacy for use in short-duration test facilities such as shock tunnels.

Acknowledgements

This work was supported by the National Research Foundation of Korea (NRF) grant funded by the Korea government (MSIT) (No: NRF-2018M1A3A3A02065959).

References

1. Park, G., “Oxygen Catalytic Recombination on Copper Oxide in Tertiary Gas Mixtures.” Journal of Spacecraft and Rockets, Vol. 50, No. 3, pp. 540-555, 2013, doi:10.2514/1.A32312.
2. Cheung, T. M., Schrijer, F. F. J., and Park, G., “Nitrogen Catalytic Recombination on Copper Oxide in Tertiary Gas Mixtures.” Journal of Spacecraft and Rockets, Vol. 53, No. 4, pp. 644-653, 2016, doi: 10.2514/1.A33512.
3. Jo, S. M., Shim, H., Park, G., Kwon, O. J., and Kim, J. G., “Temperature Determination in a Shock Tube Using Hydroxyl Radical A-X Band Emission.” Physics of Fluids, Vol. 31, pp. 791-797, 2019, doi: 10.1063/1.5082240.
4. Kim, I., Park, G., and Na, J. J., “Experimental Study of Surface Roughness Effect on Oxygen Catalytic Recombination.” International Journal of Heat and Mass Transfer, Vol. 138, pp. 916-922, 2019, doi: 10.1016/j.ijheatmasstransfer.2019.04.049.

5. Caller, A., "Comparison of Thin Film Resistance Heat Transfer Gauges in Shock Tunnel Analysis." Bachelor's Thesis, The University of Queensland, Australia, 2001.
6. Lee, S., Oh, B.-S., Kim, Y., and Park, G., "High-Altitude Environment Simulation of Space Launch Vehicle Including a Thruster Module." Journal of the Korean Society for Aeronautical and Space Sciences, Vol. 46, No. 10, pp. 791-797, 2018, doi:10.5139/jksas.2018.46.10.7 91.
7. Park, G., Park, C., Jin, Y., Choi, H., Byun, J., and Hwang, K., "Ethylene Transverse Jets in Supersonic Crossflows." Journal of Propulsion and Power, Vol. 31, No. 3, pp. 773-788, 2015, doi: 10.2514/1.B35323.
8. Chang, W. K., Park, G., Jin, Y., and Byun, J., "Shock Impinging Effect on Ethylene Flameholding." Journal of Propulsion and Power, Vol. 32, No. 5, pp. 1230-1239, 2016, doi:10.2514/1.B36007.
9. Chang, E. W. K., Yang, S., Park, G., and Choi, H., "Ethylene Flame-Holding in Double Ramp Flows." Aerospace Science and Technology, Vol. 80, pp. 413-423, 2018, doi:10.1016/j.ast.2018.07.012.
10. Kim, K., Park, G., and Jin, S. "Flameholding Characteristics of Ethylene-Fueled Model Scramjet in Shock Tunnel." Acta Astronautica, Vol. 161, pp. 446-464, 2019, doi:10.1016/j.actaastro.2019.02.022.
11. Lee, S., Song, H., Park, G., and Lee, J. K., "Freefalling Heated Sphere in a Shock Tunnel." AIAA Journal, Vol. 55, No. 11, pp. 3995-3998, 2017, doi:10.2514/1.J055967.
12. Kim, I., Lee, S., Park, G., and Lee, J. K., "Overview of Flow Diagnosis in a Shock Tunnel." International Journal of Aeronautical and Space Sciences, Vol. 18, No. 3, pp. 425-435, 2017, doi: 10.5139/IJASS.2017.18.3.425.
13. Tanno, H., Komuro, T., Lillard, R. P., and Olejniczak, J., "Experimental Study of High-Enthalpy Heat Flux Augmentation in Shock Tunnels." Journal of Thermophysics and Heat Transfer, Vol. 29, No. 4, 2015, pp. 858-862, doi:10.2514/1.T4478.
14. Park, G., Gai, S. L., and Neely, A. J., "Laminar Near Wake of a Circular Cylinder at Hypersonic Speeds." AIAA Journal, Vol. 48, No. 1, pp. 236-248, 2010, doi:10.2514/1.44167.
15. Irimpan, K. J., and Menezes, V., "Effect of Surface Roughness on the Heating Rates of Large-Angled Hypersonic Blunt Cones." Acta Astronautica, Vol. 144, pp. 331-338, 2018, doi:10.1016/j.actaastro.2018.01.011.
16. Kumar, R., "Design, Fabrication and Novel Calibration Techniques for Heat Transfer Gauges During Short-Duration Transient Measurement." Ph.D Dissertation, Indian Institute of Technology Guwahati, India, 2014.
17. Kumar, R., and Sahoo, N., "Dynamic Calibration of a Coaxial Thermocouples for Short Duration Transient Measurements." Journal of Heat Transfer, Vol. 135, No. 12, pp. 1-7, 2013, doi:10.1115/1.4024593.
18. Manjhi, S. K., and Kumar, R., "Stagnation Point Transient Heat Flux Measurement Analysis from Coaxial Thermocouples." Experimental Heat Transfer, Vol. 31, No. 5, pp. 405-424, 2018, doi:10.1080/089161 52.2018.1431738.
19. Menezes, V., and Bhat, S., "A Coaxial Thermocouple for Shock Tunnel Applications." Review of Scientific Instruments, Vol. 81, No. 10, pp. 104905, 2010, doi:10.1063/1.3494605.
20. Coblish, J., Coulter, S., and Norris, J., "Aerothermal Measurement Improvements Using Coaxial Thermocouples at AEDC Hypervelocity Wind Tunnel No. 9." AIAA 2007-1467, Reno, Nevada, US, 2007.
21. Kumar, M. D., "To Develop a Coaxial Thermocouple Sensor for Temperature Measurement in Shock Tube." International Journal of Advanced Information Science and Technology, Vol. 27, No. 27, pp. 64-68, 2014, DOI:10. 15693/ijaist/2014.v3i7.81-85.
22. Irimpan, K. J., Mannil, N., Arya, H., and Menezes, V., "Performance Evaluation of Coaxial

Thermocouple Against Platinum Thin Film Gauge for Heat Flux Measurement in Shock Tunnel." Measurement, Vol. 61, pp. 291-298, 2015, doi: 10.1016/j.measurement. 2014.10.056.

23. Mohammed, H., Salleh, H., and Yusoff, M. Z., "Design and Fabrication of Coaxial Surface Junction Thermocouples for Transient Heat Transfer Measurements." International Communications in Heat and Mass Transfer, Vol. 35, No. 7, 2008, pp. 853-859. doi:10.1016/j.icheatmasstransfer.2008.03. 009.
24. Mohammed, H. A., Salleh, H., and Yusoff, M. Z., "Dynamic Calibration and Performance of Reliable and Fast-Response Coaxial Temperature Probes in a Shock Tube Facility." Experimental Heat Transfer, Vol. 24, No. 2, 2011, pp. 109-132. doi:10.1080/ 0891615 2.2010.482752.
25. Marineau, E., and Hornung, H., "Modeling and Calibration of Fast-Response Coaxial Heat Flux Gages." AIAA 2009-737, Orlando, Florida, US, 2009.
26. Agarwal, S., Sahoo, N., and Singh, R. K., "Experimental Techniques for Thermal Product Determination of Coaxial Surface Junction Thermocouples During Short Duration Transient Measurements." International Journal of Heat and Mass Transfer, Vol. 103, pp. 327-335, 2016, doi: 10.1016/j.ijheatmasstransfer.2016.07.062.
27. Sanderson, S. R., and Sturtevant, B., "Transient Heat Flux Measurement Using a Surface Junction Thermocouple." Review of Scientific Instruments, Vol. 73, No. 7, 2002, pp. 2781-2787. doi:10.1063/ 1.1484255.
28. Jessen, C., Vetter, M., and Grönig, H., "An Experimental Investigation of Surface Thermometry and Heat Flux." Zeitschrift für Flugwiss, Weltraumforsch, Vol. 17, 1993, pp. 73-81.
29. Coker, A. K., "Ludwig's Applied Process Design for Chemical and Petrochemical Plants." Gulf Professional Publishing, 2010.
30. Schultz, D. L., and Jones, T. V., "Heat-Transfer Measurements in Short-Duration Hypersonic Facilities." AGARDograph, Vol. 165, 1973.
31. Kim, K., and Park, G., "Study of Test Time Extension in KAIST Shock Tunnel." Journal of Propulsion and Energy, Vol. 1, No.1, pp. 11-23, 2020.
32. Yang, Y., Kim, I., and Park, G., "Experimental and Numerical Study of Oxygen Catalytic Recombination of SiC-Coated Material." International Journal of Heat and Mass Transfer, Vol. 143, pp. 118510, 2019, doi:10.1016/j.ijheatm asstransfer.2019.118510.